

Superposed folding at the junction of the inland and coastal belts, Damara Orogen, NW Namibia

Adam C. Maloof

Department of Earth and Planetary Sciences, Harvard University, 20 Oxford Street, Cambridge, MA 02138, maloof@fas.harvard.edu

Two adjoining dome structures in Neoproterozoic Otavi Group sediments are located at the intersection of the Outjo (inland branch) and Kaoko (coastal branch) fold and thrust belts of the Damara Orogen on the farm Vrede, northwestern Namibia. Systematic mapping of outcrop-scale cleavage and folding relationships has unraveled three temporally distinct folding events in the two dome structures. In present-day coordinates, the first shortening event (D_1) produced E-W trending folds. The second contractional phase (D_2) developed N-S trending folds. The third shortening episode (D_3) featured a renewed production of E-W trending folds. If this chronology of deformation is applied to similarly oriented structures along the inland and coastal belts, a history of ocean closure and the amalgamation of southwestern Gondwanaland can be inferred. Closure of the Adamastor ocean and collision along the Kaoko margin began before closure of the Khomas sea and collision along the inland belt.

Introduction

The Vrede domes are a pair of doubly plunging anticlines located on Vrede farm, at the junction of the Pan-African age (650-450 Ma) Outjo fold and thrust belt (Northern Zone of the inland branch in Miller (1983)) and Kaoko fold and thrust belt (Central Kaoko Zone of the coastal branch in Miller (1983); Fig. 1). Doming has been recognized as a prevalent feature of the Outjo thrust belt (Frets, 1969; Miller, 1983; Weber *et al.*, 1983) and Swakop zone (Smith, 1965, Barnes and Downing, 1979; Miller, 1983; Kröner, 1984; Oliver, 1995; Fig. 1). Kröner (1984) proposed that late-tectonic, anatectically produced granites intruded and ballooned into preexisting anticlines in the cover sediments of the Swakop zone, producing domes. Further north in the area of the Vrede domes, the Outjo thrust belt is riddled with post-tectonic granites (520-500 Ma) and the diapir mechanism for dome formation appears plausible. Superposed tectonic folding has also been evoked

as a mechanism for doming in the Swakop zone (Smith, 1965) and Outjo thrust belt (Frets, 1969; Miller, 1983). In theory, two orthogonally-oriented fold trains should interact like waves to form basin and dome fold interference patterns (Ramsay, 1958, 1962; Weiss, 1959; Tobisch, 1966; Ghosh, 1970; Watkinson, 1981; Theissen, 1986; Ramsay and Huber, 1987; Lisle *et al.*, 1990). In the Swakop zone, the dearth of outcrop-scale refolded structures has usually led to the adoption of the diapir model (Barnes and Downing, 1979; Kröner, 1984). A third mechanism for dome formation has been proposed for the Swakop zone involving oblique collision and lateral tectonic escape along mid-crustal ductile detachments (Oliver, 1995). This model is probably not applicable to the lower-grade rocks of the Outjo thrust belt.

The Vrede domes are low-grade, thin-skinned structures containing a plethora of outcrop-scale refolded folds and multiply deformed axial-planar cleavages. The goal of this contribution is to deconvolve the refolded folds of the domes into chronologically distinct components of finite strain. Four models are presented to explain the structural evolution of the domes. The chronology of deformation in the domes is then used to speculate on the relative timing of ocean closure along the inland and coastal belts during the amalgamation of southwestern Gondwanaland.

Geologic Setting

The Vrede domes consist of two northeast verging domal anticlines that are separated by an east-west trending keel-shaped syncline (Fig. 2). The domes owe their ring-like appearance in plan view to a drainage network that follows the weakest Otavi stratigraphy (Ghaub Formation and Lower Ombombo Subgroup siltstones), eroding circular, low-order channels that eventually feed higher order ephemeral streams which drain into the Huab River. The domes are each about 1.5 km wide (east-west), and together they are about 4 km long (north-south).

The domes lie in the Huab River channel, which drains the southwest heel of the Kamanjab Inlier (1.7-2.0 Ga basement; Fig. 1). Cretaceous volcanics related

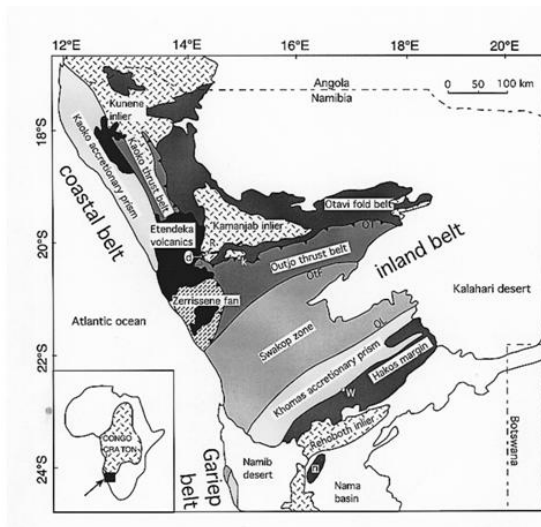


Figure 1: Tectonostratigraphic map of NW Namibia (after Frets, 1969; Miller, 1983; Hoffmann, 1983, 1989; K-H Hoffman (unpublished)): d: Vrede domes, R: Rockeys fault, n: Naukluff klippe, OT: Outjo thrust, OF: Otjohorong fault, OL: Oka-handja lineament, k: town of Khorixas, W: city of Windhoek.

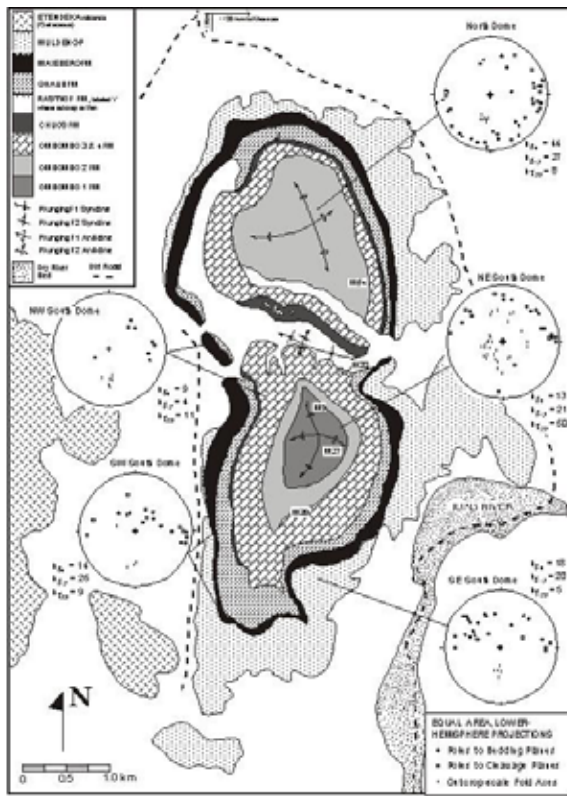


Figure 2: Geological map of the Vrede domes. FM: Formation, GP: Group, M#: locality referred to in text.

to the opening of the Atlantic Ocean occur west and south of the Vrede domes and post-tectonic (~500 Ma) granites border them to the southeast (Fig. 1).

Regional Tectonostratigraphy

The Otavi Group is a carbonate-dominated passive-margin succession bordering the southern promontory of the Congo Craton (of which the Kamanjab Inlier is a part). The megasequence records the ~750 Ma breakup of the supercontinent Rodinia, a stable platform with two discrete glacial intervals capped by distinctive Neoproterozoic cap carbonates (Fairchild, 1993; Schmidt and Williams, 1995; Kennedy, 1996; Hoffman *et al.*, 1998a; Kennedy *et al.*, 1998), and the ~550 Ma amalgamation of Gondwanaland (Fig. 3b; Hoffman *et al.*, 1998D). The Otavi Group is underlain by pre-760 Ma Nosib Group syn-rift clastics and a low grade, 2.0-1.7 Ga basement complex. It is overlain by pre-540 Ma Mulden Group foreland basin siliciclastics (Frets, 1969; Hoffman *et al.*, 1998D).

The Otavi passive margin is segmented into basins by transverse basement ridges (Henry *et al.*, 1990). Henry *et al.* (1990) and Stanistreet *et al.* (1991) have suggested that much of the early rifting was controlled by large, low-angle detachments that exploited older, Mesoproterozoic structures. The Otavi rocks of the Vrede domes are located south of the Huab Ridge, the southernmost transverse basement ridge, and south of Rockeys Fault

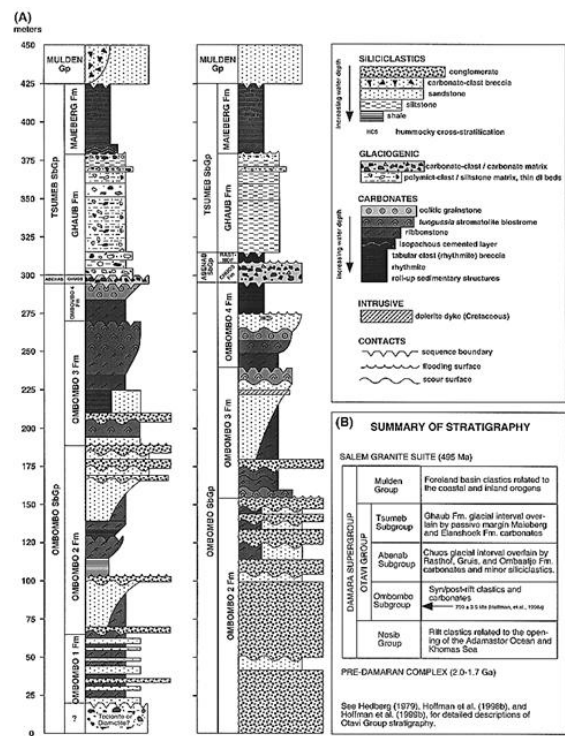


Figure 3: (a) Stratigraphic columns for the South and North domes. Fm: Formation, Gp: Group, SbGp: Subgroup; (b) Summary of Otavi Group Stratigraphy.

(Fig. 1). Henry *et al.* (1990) proposed that the Rockeys fault is the northernmost extensional detachment and the postulated shelf-slope transition bounding the Otavi platform to the north.

The Stratigraphy of the Vrede domes

In the Vrede domes, the Otavi Group is a 400+ m sequence of carbonates and siliciclastic metasediments, variably folded and metamorphosed to lower greenschist facies. Figure 2 is a geologic map of the Vrede structures, and Figure 3 provides stratigraphic columns for each dome.

The Ombombo Subgroup forms the bulk of the Vrede stratigraphy. The southern dome is cored by 50+ m of Ombombo-1 Formation (Fm.) black-maroon limestones (partially dolomitized) and sandstones. The limestones/dolostones of this unit form the resistant ridges that contain metre-scale refolded folds at location M9 (Fig. 2). A 15+ m thick lens of diamictite/tectonite lies in the hinge of a 150 m wavelength, E-W trending fold at M9. The northern dome shows less structural relief than the southern dome and does not expose Ombombo-1 Fm. rock.

The Ombombo-2 Fm. varies significantly across the domes. In the northern dome, the Ombombo-2 Fm. is a 100+ m thick unit of nearly continuous coarse-grained, polymictic conglomerate (Maloof, 1998), broken only by thin sandstone beds and rare dolostone ribbon beds. In the southern dome, the Ombombo-2 Fm. contains

thin, medium-grained conglomerate beds separating thicker beds of fine-medium sandstone and dolostone ribbons.

The Ombombo-3 and Ombombo-4 Fm. are lithologically consistent across the domes, displaying two or three parasequences containing pinkish red *Tungussia* stromatolite biostromes (Semikhatov, 1962) with ooids and dolostone ribbons. The silicified ooid beds lie parallel to bedding and serve as useful marker horizons. A volcanic ash layer near the top of Ombombo-3 in a stratigraphically correlative section 150 km to the north has a U-Pb zircon age of 759 ± 3.5 Ma (Fig. 3; Hoffman *et al.*, 1998D).

The Abenab Subgroup is extremely thin in the Vrede domes. The Chuos Fm. glaciogenic diamictite marks the base of the Abenab Subgroup and rests unconformably on the Ombombo-4 Fm. Without the presence of the overlying Rasthof Fm., the Chuos Fm. cannot be distinguished conclusively from the overlying Ghaub diamictite of the Tsumeb Subgroup. However, where the Rasthof Fm. is present, the Chuos Fm. is a pink-grey, carbonate-clast, carbonate-matrix diamictite with very rare striated basement clasts. For the Rasthof Fm., only the lowermost 4 m of black, finely laminated rythmites with rollover algal mats was preserved prior to the downcutting of the Ghaub glaciation (Fig. 3).

The Ghaub Fm. marks the base of the Tsumeb Subgroup and cuts into the Abenab and Ombombo Subgroups creating an unconformable contact with 6+ m of local relief. The Ghaub Fm. is a glaciomarine diamictite characterized by large (up to 2 m diameter) carbonate and basement granitoid/gneiss dropstones within a fine siltstone or carbonate matrix. In the northern dome, the unit contains only rare <5 cm diameter dropstones in the siltstone diamictite, while in the southern dome, the unit is packed with large and lithologically diverse dropstones.

Along the western edge of the Vrede domes, an up to 2.8 m thick green ash bed occurs between the Ghaub and the Maieberg Formations. The ash is silicified and ferruginized, perhaps because of its proximity to the Mulden-Tsumeb exposure surface. Four zircon grains were separated from the ash unit for U-Pb geochronology. Unfortunately, the grains gave upper concordia intercept ages of 1.7-1.9 Ga and lower intercept ages of 0.51-0.52 Ga (S.A. Bowring, pers. com., 1998). The zircons are probably detrital grains that were affected by Pan-African Pb-loss.

Where the ash unit is not present, the Ghaub Fm. grades almost conformably into Maieberg Fm. dolostone rythmites characterized by distinctive undulating waves of 0.5-2 cm wide isopachous cement, 10-200 cm in wavelength and 5-100 cm in amplitude. The Maieberg cement layer grades into variably dolomitized limestone rythmites, followed by massive recrystallized dolomite with calcite vugs up to 1 m in diameter.

The outermost shell of the Vrede domes consists of Mulden Gp. siltstones, phyllites, quartzites, feldspathic

quartz arenites, quartz-pebble conglomerates and dolomite-clast breccias. A highly ferruginized and silicified subaerial unconformity is present where the Mulden Group truncates the Maieberg Formation.

The Structure of the Vrede domes

At the map-scale, 1-2 km wavelength folding of the thick and competent Ombombo 2, 3, 4 Fm. conglomerates and dolostones created a 1.5 km wide and 4 km long pair of lobate domes separated by a keel-shaped synclinal basin (Fig. 2). Associated Otavi Group siltstones and fine-grained sandstones are deformed more passively around folded dolostone and conglomerate horizons, leading to map-scale layer thickness variations in the less competent units. The less competent siltstone and limestone units contain the metre-scale, multiply deformed folds and cleavages that are the subject of the remainder of this paper.

Cleavage

The Otavi Group carbonates rarely preserve a cleavage, and when they do, it is spaced, discontinuous and often just a series of stylolitic discolorations (Alvarez *et al.*, 1976). The carbonates never contain two cleavages in hand sample. Fortunately, the Ombombo carbonates are closely associated with siltstones and sandstones that contain one and often two sets of penetrative cleavage. In some localities, the intersection of the two cleavages leads to typical pencil-shaped debris (e.g. M9). In other locations, the cleavages interact to create an older, tightly spaced crenulation cleavage accommodating large amounts of strain, and a younger, spaced, planar cleavage accounting for relatively less volume loss (e.g. M20). Occasionally, a thin sandstone or dolostone bed within a siltstone matrix will preserve a fold train that displays the geometric and chronologic relationship between the folds and the cleavages.

Cleavage formation in the Otavi rocks of the Domes was accomplished, at least partially, by pressure dissolution. Even in siltstones, insoluble clay and iron residues remain on the cleavage surface and no mica growth is visible. The older cleavage tended to remove the soluble material to accommodate shortening, making it difficult for the younger cleavage to develop because of the dearth of water and soluble minerals after the first deformation. However, when one of the two cleavages is not present, the cleavages are not physically distinctive in hand sample. Quartz veins are often present, but it is difficult to tell whether they represent reprecipitation of material mobilized by pressure dissolution, or whether they are related to other processes.

If granite diapirism was the cause of doming, a single, nearly horizontal cleavage inclined away from the core of the dome would be expected. The common occurrence of two sets of mutually perpendicular penetrative cleavage, each set axial-planar to a group of physically

distinct folds, supports the multiple-event, superposed folding hypothesis. Outcrop-scale relationships between multiple cleavages shed light on the sequence of deformational events within the Vrede domes.

Outcrop-scale evidence of three discrete folding events

Siltstones along the central north-south axes of the Vrede domes tend to preserve two cleavages. The two cleavages intersect at 80-90° and display obvious cross-cutting relations. The S₁ cleavage is tightly spaced, penetrative and generally strikes E-W. The S₂ cleavage is widely spaced (up to 1-2 cm), nearly planar, variably penetrative strikes consistently ~160° and dips ~60°. At M20 (Fig. 2) and in the region along the axis of the keel-shaped syncline, S₁ is sheared into S-shaped micro-folds between the S₂ cleavage (Fig. 4). Towards the east and west flanks of the domes, S₁ becomes discontinuous and eventually disappears, while S₂ becomes progressively more closely spaced and continuous.

It is possible to assign both S₁ and S₂ to a distinct set of folds (F₁ and F₂ respectively), based on axial-planar cleavage relationships. Measurable F₁ folds are rare, but where preserved, appear as stranded dolostone hinge zones ~5-20 m across with attenuated limbs (Fig. 5). F₁ folds trend approximately E-W to ENE-WSW, verge to the north, and are gently (0-20°) plunging (Fig. 7b). Without exception, the F₁ folds preserve relatively undisturbed axial-planar S₁ in their hinges, while S₁ is either crenulated by S₂ or not present at all outside of the hinge zones (Fig. 5). S₂ transects both limbs of F₁ folds (Fig. 5, 7c). F₁ folds are best developed along the N-S central axis of the domes (e.g. M20, M9).

F₂ folds are variable in style but are always smaller in scale, more regularly developed throughout the domes and more steeply plunging than F₁. For example, at M9, F₂ form as 0.5-2 m wavelength N-S trending folds

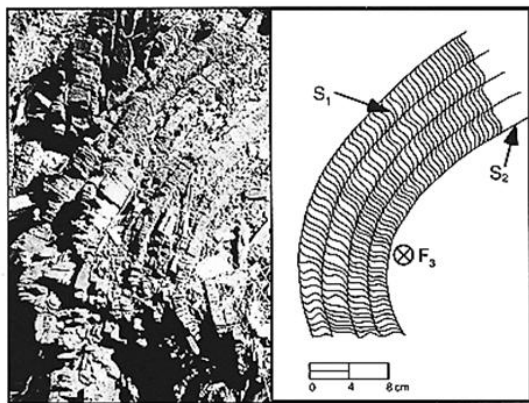


Figure 4: Thick siltstone unit located at M20. Bedding (S₀) is at an angle to both S₁ and S₂, though S₀ is difficult to see in this outcrop. S₁ is a closely-spaced cleavage sheared into sigmoidal micro-folds between the younger, widely-spaced S₂ cleavage planes. S₁ was sheared by flexural slip between S₂ layers when S₂ was broadly folded by D₃. The crosshair marks an F₃ fold axis going into the page.

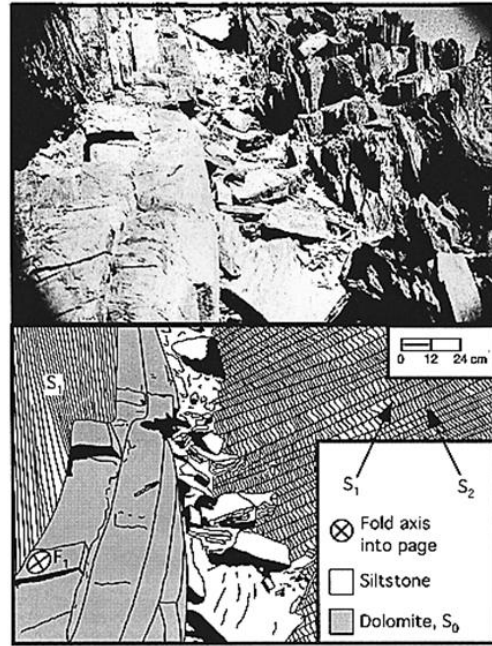


Figure 5: Isolated E-W trending F₁ fold hinge zone (marked by crosshair) and attenuated limb in Ghaub Fm. dolostone layer at M20. Within the siltstone inside the hinge zone (upper left corner of figure), the S₁ cleavage is undisturbed and axial-planar to the F₁ fold. In the siltstone outside the hinge zone (right side of figure), S₁ is crenulated by a more widely spaced S₂ cleavage that intersects S₁ at a 90° angle and transects both limbs of the F₁ fold.

in the attenuated limbs of a 50 m wavelength F₁ fold train (Fig. 7c). In thick siltstones, where there are no competent dolostone horizons, F₂ deforms S₁ into 0.25-1 m wavelength N-S trending folds. The F₂ folds exploit the more regular and closely spaced S₁ fabric for layer-parallel slip, deforming the original bedding planes as passive markers (Figs. 6, 7b, c).

In rare locations, clustered in the region of the keel-shaped syncline (M20, M54), entire outcrops of F₁ and F₂ folded massive siltstone are refolded into broad, 5 m-wavelength, 1 m-amplitude, E-W trending, N-verging folds (F₃). During F₃ folding, flexural slip along the S₂ planes sheared S₁ planes into sigmoidal microfolds (Fig. 4).

Summary of deformational history

Three discrete deformational events are visible at outcrop-scale (D₁, D₂, and D₃; Table 1). The chronology of deformation recorded at outcrop-scale is assumed to be consistent with, and representative of, the map-scale structural history (Ramsay and Huber, 1987; Davis and Reynolds, 1996, Passchier and Trouw, 1996). This approach is supported by the similarities in the relative orientation of cleavages with respect to outcrop-scale and map-scale folds.

It is interesting to note that none of the outcrop-scale structures show the Type-1 basin and dome interference pattern so obvious in the map-scale expression of the

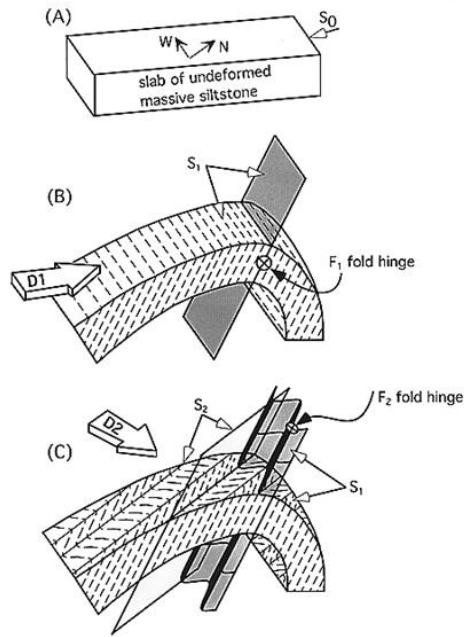


Figure 7: Model for the kinematics of outcrop-scale D_1 and D_2 folding in less competent units: (a) Undeformed slab of massive siltstone (S_0 is bedding); (b) D_1 deforms S_0 into open, E-W trending, N-vergent, gently plunging F_1 folds with S_1 axial-planar cleavage; (c) During D_2 , the tightly-spaced S_1 cleavage is deformed into steeply plunging F_2 layer-parallel slip folds while S_0 is deformed as a passive marker. The plunge of the F_2 folds is determined by the dips of the S_1 cleavage planes, which are in turn related to the vergence of the F_1 fold and to the degree of fanning in the S_1 cleavage. Note: map-scale folding was controlled by thick competent units such as the Ombombo 3-4 Fm. carbonates. Therefore, during D_2 , S_0 remained the fabric along which layer-parallel slip was accomplished. The resulting map pattern reflects the basin and dome architecture typical of orthogonally interfering deformation fronts (see Ramsay, 1958, 1962; Weiss, 1959; Tobisch, 1966; Ghosh, 1970; Watkinson, 1981; Theissen, 1986; Ramsay and Huber, 1987; Lisle *et al.*, 1990).

thick competent units such as the Ombombo 2, 3 and 4 Fm. that control the geometry of the Vrede structures (Fig 2). Younger deformations in less competent siltstones exploit a tectonically developed set of nearly uniformly dipping layers (S_1) rather than the primary bedding (S_0) (Figs. 4, 5 and 6). In Figure 7, a model is

presented for the sequence of contractional events that may be representative of outcrop-scale deformation in less competent units throughout the domes.

Implications for Regional Tectonics

Tectonic Setting

The Damara-Kaoko-Gariep Orogen is a late Pan-African (560-500 Ma) trench-trench-trench triple junction recording the simultaneous convergence of the Congo, Kalahari, and Rio de la Plata cratons (Fig. 8; Hoffman, 1996; Prave, 1996; Hoffman, 1991). Trench sedimentation (Kukla and Stanistreet, 1991), formation of the Khomas accretionary prism (Fig. 1), and south-verging fold belts (Miller, 1983) suggest that the Congo craton was the upper plate with respect to the Kalahari craton. Andean-type arc magmatism in the Camaqua retro-arc basin of southern Brazil (Gresse *et al.*, 1996) and East-verging fold belts (Germs and Gresse, 1991; Coward, 1983) suggest that the Congo craton was the lower plate with respect the Rio de la Plata craton (Fig. 8; Hoffman, 1996). Kinematic indicators imply that collisions along each arm of the triple junction were left-lateral oblique (Fig. 8, 9a; Coward, 1983). One of the major problems that remains unsolved involves the relative timing of ocean closures and continental collisions between the three plates.

The timing of continental collision between the Congo, Kalahari, and Rio de la Plata cratons

In the Vrede domes, outcrop-scale crosscutting relationships between genetically linked folds and cleavages have distinguished a chronological sequence of deformational events for the domes (Table 1). In order to attach these phases of deformation to specific tectonic events, structures in the Vrede domes are linked with previous fold/cleavage style and relative timing observations from structures along the Outjo and Kaoko thrust belts (Table 2). Then, the change in strength of each chronologically distinct set of structures with their relative distance from the inland and coastal de-

Table 1: Summary of the chronology and style of deformation in the Vrede domes.

Deformational Phase	Outcrop-scale style of deformation	Map-scale expression (interpretation)
D_1	Large (5-100 m wavelength) E-W trending, shallowly plunging open folds (F_1) and a well-developed, steeply dipping, closely spaced axial-planar cleavage— F_1 and S_1 are typically strongly refolded/rotated by D_2 .	Folded Otavi Gp. sediments into a broad E-W trending anticline-syncline-anticline train with cusped-lobate geometry.
D_2	Small (0.5-2 m wavelength), tight, steeply plunging, N-S trending folds (F_2) in S_1 layering. F_2 folds are associated with a variably spaced axial-planar cleavage that dips to the west— F_2 and S_2 are consistently oriented throughout the domes and are rarely deformed by D_3 .	Folded E-W trending anticline-syncline-anticline into a Type-1 NE-verging basin and dome structure (Fig. 2). The Type-1 two-dimensional interference pattern is the result of discrete D_1 and D_2 buckling phases interfering at nearly 90° angles (Ramsay, 1967; Theissen, 1980; Theissen, 1986).
D_3	Rare E-W trending open F_3 folds—style and degree of development vary over short distances due to the complex structural grain that had developed after D_1 and D_2 . Renewed slip along S_2 planes shears S_1 planes into sigmoidal micro-folds.	Pushed southern dome further into northern dome asymmetrically, squeezing intervening syncline into the shape of a keel and developing northern sense of vergence in both domes.

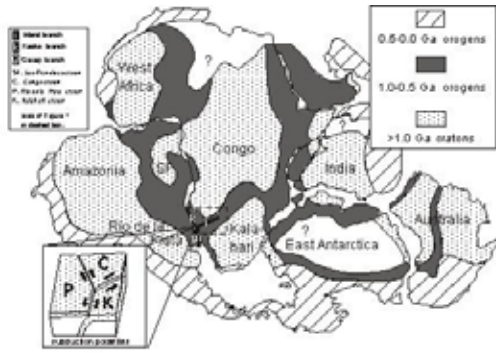


Fig. 8

Figure 8: Pan-African orogens related to the assembly of Gondwanaland (after Hoffman *et al.* 1999b and references therein; Kröner, pers. com., 1999): The domes are located at the junction of the Kaoko (coastal) and Damara (inland) belts, between the Congo, Rio de la Plata, and Kalahari cratons. The Gariep belt separates the Kalahari and Rio de la Plata cratons and joins the coastal and inland belts to form the third arm of the triple junction. The Congo craton was the upper plate with respect to the Kalahari craton but was the lower plate with respect to the Plata craton. Subduction along each boundary was accompanied by a component of left-lateral slip. SF: Sao Francisco craton.

formation fronts will suggest which tectonic event is responsible for each set of structures.

Along the coastal belt, Coward (1981) identified predominantly N-S trending structures in the north which experience an abrupt 90° change in trend near Khorixas (Fig. 1), about 120 km east of the Vrede domes. The NE-SW (D₁) and N-S (D₂) trending structures weaken systematically to the east (Coward, 1983) and D₁ structures appeared before collision along the inland branch began (Miller, 1983). Therefore, it is suggested that D₁ and D₂ structures are related to deformation focussed along the coastal belt associated with closure of the Adamastor ocean.

In the Vrede domes and further east in the Outjo thrust belt (Miller, 1983; Coward, 1983), D₁ and D₂ were

weakly deformed by an E-W trending D₃. Southeast of the domes within the Swakop zone of the inland belt, intense N-S directed shearing and folding are observed to rework an older structural grain (D₁ + D₂ ?; Coward, 1983; Miller, 1983; Porada *et al.*, 1983). Coward (1983) and Stanistreet *et al.* (1991) noted that the intensity of this deformation weakens rapidly with distance from the inland belt and attribute the shortening to the closure of a narrow (Meert *et al.*, 1995) Khomas sea. Coward (1981) concluded that deformation related to the closure of the Khomas sea is present only as a weak E-W trending overprint along the southwestern margin of the Congo craton (including the Vrede area). Therefore, D₃ in the Vrede domes likely represents a distal pulse of N-S shortening related to the collision of the Congo and Kalahari cratons.

The proposed chronology is consistent with ⁴⁰Ar/³⁹Ar mineral cooling histories extracted from the 547-543 Ma Gariep belt (Frimmel and Frank, 1998). The tectono-thermal evolution of the Gariep belt suggests earliest closure of the northern Adamastor Ocean, followed by destruction of the Khomas Sea, and succeeded by closure of the southern Adamastor ocean (Gariep belt) (Frimmel and Frank, 1998). Tectonostratigraphic studies within the Damaran Orogen, however, suggest that either the Khomas sea closed before the Adamastor ocean (Stanistreet *et al.*, 1991) or vice versa (Prave, 1996).

The evolution of the stress field at the junction of the coastal and inland belts

Why did ocean closure along the nearly N-S oriented Kaoko margin give rise to an initial phase of locally E-W trending structures (e.g. in the Vrede domes) followed by the development of N-S trending structures? Coward (1981) did not recognize a consistent interference pattern between the two structural trends, and considered the entire coastal belt to represent a single

Table 2: Synthesis of timing-of-deformation data from the Outjo and Kaoko thrust belts. D_# in the left column are deformation episodes referred to in this contribution. D₀ is not discussed further because there is no evidence for pre-Mulden deformation in the Vrede domes. D_# enclosed in parentheses within each entry of the table are the deformation episode labels used by the authors in previous publications.

	Frets (1969), Miller (1983)--Outjo thrust belt.	Coward (1983)--Outjo and Kaoko thrust belts.	Porada (1989)--Outjo thrust belt and Zerrissene fan.	This paper--the junction of the Outjo and Kaoko thrust belts.
D ₀	Local. Open to tight, upright to northward verging, E-W trending folds pre-dating Mulden Gp. deposition. (D ₁)		Bedding-parallel cleavage formation pre-dating Mulden Gp. deposition. (D ₁)	
D ₁	Regional. Cleavage forming event. Fold orientations controlled by the shapes and locations of basement inliers. Post-dates Mulden Gp. deposition. Attributed to pre-collisional deformation along inland belt. (D ₂)	NE-SW trending, SE-verging asymmetric folds. Deformation strengthens significantly in the Kaoko thrust belt to the north along the coastal belt. (K ₁)	NE-SW trending structures post-dating Mulden Gp. deposition. (D ₂)	E-W trending folds and discontinuous axial-planar cleavage post-dating Mulden Gp. deposition.
D ₂	N-S folds and vertical cleavage of the Zerrissene fan. Effects of this deformation die out rapidly to the East. (D ₃)	N-S trending, W-verging chevron folds. Greenschist facies metamorphism. Fold tightness and asymmetry decrease rapidly to the East. (K ₂)	N-S trending, W-verging folds post-dating 570 Ma granite intrusions. (D ₃)	N-S trending, E verging folds and almost ubiquitous axial-planar cleavage.
D ₃	Gentle, ENE-WSW trending folds and vertical cleavage. Post-dates the Salem granite intrusion (495 Ma). (D ₄)	NE-SW trending upright crenulations. (K ₃)		Weak ENE-WSW trending folds and no cleavage development.

phase of differential shortening related to the closure of the Adamastor ocean and continental collision along the coastal belt. Coward (1981) went on to suggest that the change in structural trend was related to the tectonic evolution of the inland branch. During ongoing collision along the coastal belt, northward subduction of the Khomas sea commenced (Fig. 9a). Subduction of the Khomas sea ocean floor beneath the Congo craton generated large volumes of granite in the Swakop zone and the Outjo thrust belt (Fig. 1). Heat from the intruded granite weakened the lithosphere along the inland branch. This weakening of the southern margin of the Congo craton led to differential E-W ductile shortening and a counterclockwise rotation of structural trends (Fig. 9b). This interpretation then predicts that D_1 was E-W directed and that ongoing deformation led to a 90° counterclockwise rotation of originally N-S trending D_1 structures (Fig. 9b). Thus, D_2 would represent a renewed pulse of E-W directed shortening, refolding the E-W trending D_1 structures across N-S trending axes. This model is consistent with the observation that D_1 structures are only locally E-W trending (Coward, 1983) and that D_1 structural orientations are frequently controlled by the shape and location of basement inliers which may have acted as individual rigid indentors during differential shortening. However, as Carey (1955) asserts, Coward's oroclinal explanation for the changing trend of the coastal belt would imply greater degrees of shortening and the unroofing of deeper structural levels along the southern Congo craton. The orocline hypothesis also predicts an increasing degree of horizontal extension towards the outer arc of the bend in the mountain belt. Mapping in the Swakop zone (Miller, 1983; Stanistreet *et al.*, 1991) and in the narrow NW-SE window of Otavi Group rocks just north of the Zerrissene fan (Hoffman, pers. com., 1998) does not show evidence for widely varying degrees of crustal shortening or horizontal extension.

Alternatively, a similar 90° rotation of D_1 structures in the Vrede domes region could be accomplished if the southwestern Congo craton acted as a discrete rotating crustal sliver (Freund, 1970; Nur *et al.*, 1986; Nelson and Jones, 1987; Sylvester, 1988; Fig. 9c). According to Nur *et al.* (1986), the 90° rotation of a crustal block requires that the block is bound by multiple sets of parallel strike-slip faults, where each set of faults has rotated less than 45° (Fig. 9d). The block rotation hypothesis is attractive because, unlike the orocline model, it does not predict an increasing degree of horizontal extension towards the outer arc of the bend in the mountain belt (Hoffman, pers. com., 1999). Unfortunately, such variably rotated strike-slip faults have not been observed to bound the southwestern Congo craton. A second test of the rotating crustal block or orocline hypotheses would be to document palaeomagnetic rotations by dating palaeomagnetic poles from nearby syn-tectonic granitic intrusions (e.g. Nelson and Jones, 1987; Beck, 1998).

Two other models may satisfactorily explain the ro-

tation of structural trends between D_1 and D_2 without requiring the 90° rotation of crustal elements. Most simply, McKenzie and Morgan (1969) predict that trench-trench-trench triple junctions are inevitably unstable. Using relative plate velocity vectors with directions based on the sinistral-oblique nature of convergence along each trench and with arbitrary magnitudes, Figures 9 a and e indicate that the Kaoko-Damara-Gariep triple junction is indeed unstable. As the plates move, the junction will be unable to retain its geometry and the relative motion of the plates will have to adjust accordingly (McKenzie and Morgan, 1969; Nitsuma, 1996). In order to reach a stable triple-point configuration, the Congo-Rio de la Plata plate boundary (CP) must rotate clockwise into parallelism with the Kalahari-Rio de la Plata plate boundary (KP), forming one long transform fault (Figs. 9 a and e). Perhaps the differential clockwise rotation of the three plates varied with time as the plate boundaries adjusted towards this more stable orientation. The complex evolving stress-field associated with the variable clockwise rotations of three interacting plates may have led to the 90° change in structural trend between D_1 and D_2 in the Vrede area.

A fourth explanation for changes in orientation of D_1 and D_2 structures involves the existence of an irregular coastal margin. Thomas (1983, 1990) used the southern Appalachian example to describe how the trace of an orogenic belt may be inherited from the geometry of the earlier rifted margin. Irregular margins composed of promontories and embayments result in diachronous collisions and rotations of the stress field (Figs. 9 f, g and h). Indeed, Porada *et al.* (1983) suggested that the Kamanjab inlier extends to the coast (Figs. 1, 9 a, f, g and h). The Kamanjab inlier (1.7-2.0 Ga basement) could act as such a cold, rigid lithospheric promontory around which the trace of Kaoko structures would rotate (Vauchez *et al.*, 1994). If the collision along the Kaoko margin closed the Adamastor Ocean like a zipper around an euler pole located well north of the Kamanjab inlier (Fig. 9a), as stratigraphic (Porada, 1989; Stanistreet *et al.*, 1991; Germs and Gresse, 1991) and $^{40}\text{Ar}/^{39}\text{Ar}$ thermochronology suggests (Frimmel and Frank, 1998), then the Kaoko collision would have begun in the north and propagated southwards (Figs. 9 a and f). Although plate convergence is E-W, the initial collision in the north (D_1) would have been strongly oblique, with a component of N-S directed stress across the WSW-ENE trending northwestern edge of the Kamanjab inlier (Fig. 9f). As the zipper closed southward beyond the NNW facing embayment and around the W-facing promontory, compressional structures (D_2) would have assumed a N-S trend (Fig. 9g).

This hypothesis can be tested directly by checking to see if the Kamanjab inlier does extend to the coast with the proposed geometry. In fact, the Zerrissene fan (Fig. 1) deposits that currently cover the alleged extension of the Kamanjab inlier are deep water turbidites that may have been deposited on oceanic crust (rather than

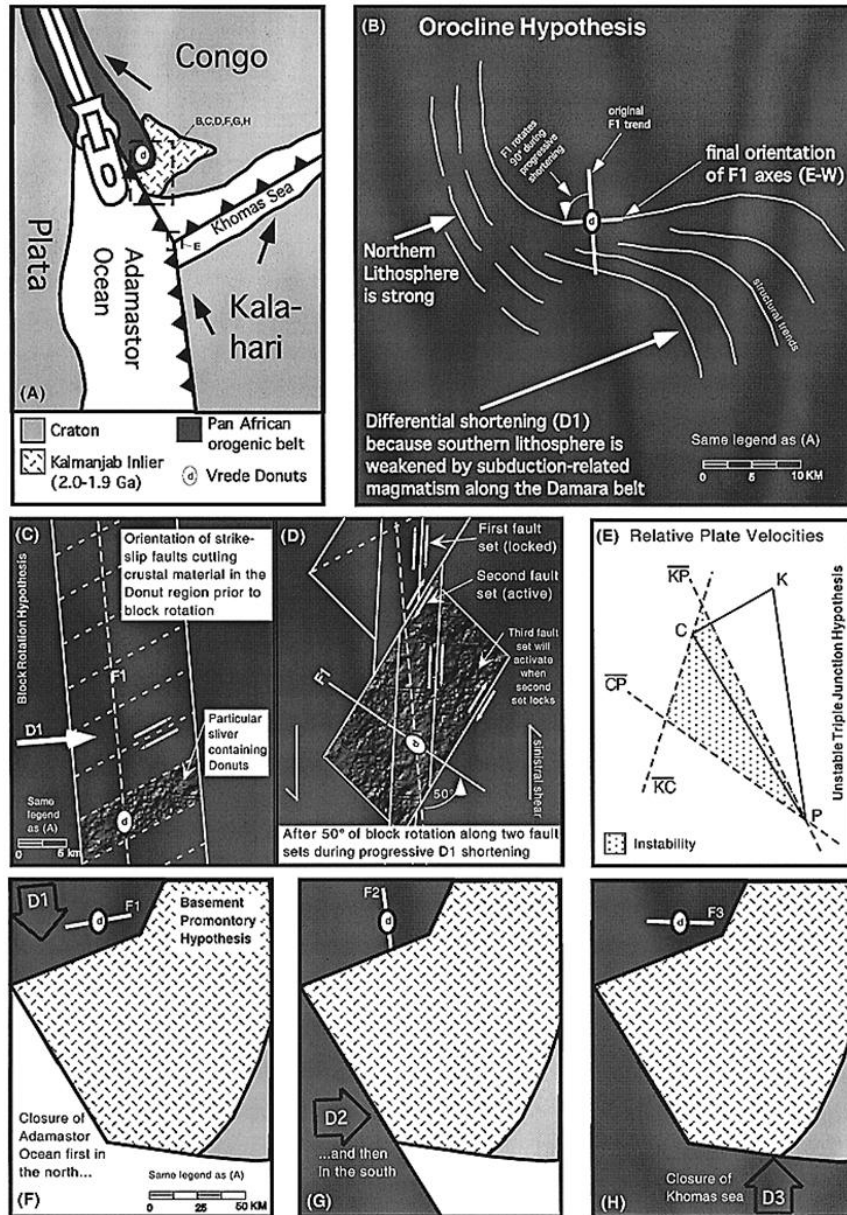


Figure 9: Models for the 90° rotation of structural trends between D₁ and D₂ during Kaoko orogenesis. The legend in (a) is relevant throughout this figure. (a) Simplified map of the triple junction between the Rio de la Plata, Congo, and Kalahari cratons. Zipper indicates diachronous E-W directed closure of the Adamastor ocean (closing progressively from north to south) around an Euler pole to the north of the diagram; (b-h) represent variable magnifications of the dome region at the junction of the inland and coastal belts (dashed boxes in (a)): (b) Orocline hypothesis (after Coward, 1981): The first phase of deformation (D₁) is E-W directed. During progressive E-W shortening, the F₁ fold axes are rotated 90° counterclockwise into shortening-parallel orientation. A second pulse of E-W directed shortening (D₂) will fold E-W trending F₁ axes across N-S trending F₂ axes; (c, d) Block rotation model (after Nur *et al.*, 1986): The first pulse of shortening (D₁) is E-W directed and forms N-S trending folds (F₁). Progressive D₁ shortening activates a set of parallel strike slip faults oriented approximately 60° from D₁ (c). Slip on the faults causes counterclockwise block rotation. The original faults will accommodate rotation until relative normal stress gets too high and slip is no longer energetically favorable. At this point, a second set of faults will form to accommodate block rotation, while the original faults lock (d). New fault sets would continue to develop until the crustal sliver that contains the domes rotated 90°. Then a second pulse of E-W shortening (D₂) would fold the E-W trending F₁ axes around N-S trending F₂ axes; (e) A representation of the triple junction in a relative plate velocity field shows that it is necessarily unstable. Assuming that the left-lateral component of slip along each plate boundary is contemporaneous, migration of the triple junction will induce clockwise rotation of the Congo craton. C: Congo craton, K: Kalahari craton, P: Plata craton, CP: Congo-Plata plate boundary, KP: Kalahari-Plata plate boundary, KC, Kalahari-Congo plate boundary; (f, g, h) The existence of a basement promontory (e.g. the southwestward extension of the Kamanjab inlier) causes a rotation of the stress field as the Adamastor ocean closes diachronously from north to south (a). The first pulse of deformation (D₁) forms E-W trending structures parallel to the north-facing edge of the Kamanjab inlier (f). The next pulse of deformation (D₂) builds N-S trending structures parallel to the west-facing edge of the Kamanjab inlier as the Adamastor ocean begins to close around the basement promontory (g). The final phase of contraction (D₃) is associated with the closure of the Khomas sea and forms E-W trending structures parallel to the southern margin of the Kamanjab inlier (h).

debris flows deposited on a basement high) (Stanistreet *et al.*, 1991). By examining Nd and Pb isotopes in syn/post-tectonic granites, we should be able to determine whether the granites traveled through 2.0-1.7 Ga granitic basement or through an accreted sliver of oceanic crust (Hoffman, pers. com., 1998).

Perhaps the boldest assumption made in this contribution and in previous work is that fold orientations and vergences describe relative plate motions and collision geometries directly. This is a risky assumption to make considering that pre-existing structure (Thomas, 1990; Vauchez *et al.*, 1994) and extensional collapse (Dewey, 1988) are only two of the many factors that may cause folds to mask true relative plate motions. Nevertheless, the striking correlation between outcrop-scale Vrede dome structures and the map-scale structures observed along the coastal and inland belts indicate that something in the tectonic evolution of NW Namibia is systematic and perhaps related directly to the relative movements of the Congo, Rio de la Plata and Kalahari plates.

Conclusions

The Vrede domes provide a rare opportunity to examine deformed Otavi Gp. sediments at the junction of the Kaoko and Damara belts. Unlike domal structures observed in the Outjo thrust belt and elsewhere in the Damara orogen, the Vrede domes are not (1) the result of post-tectonic granitic diapirism, nor are they (2) the expression of oblique convergence and lateral tectonic escape along a mid-crustal detachment. The Domes were formed by the interference of three discrete folding events, D_1 , D_2 , and D_3 . If one assumes that fold orientations and vergences are valid data for the prediction of relative plate motions, then the discrete deformational episodes in the Vrede domes suggest a chronology for the inland and coastal orogens. Coupled with structural observations from the Kaoko (Guj, 1970; Porada *et al.*, 1983, Porada, 1989; Coward, 1983; Dürr and Dingeldey, 1996) and Outjo (Frets, 1969; Porada, 1979, 1989; Porada *et al.*, 1983; Coward, 1981, 1983; Miller, 1983; Weber *et al.*, 1983) thrust belts, it is concluded that D_1 and D_2 reflect the closing of the Adamastor Ocean and subsequent Kaoko orogeny. Closure of the Khomas Sea and collision along the inland Damara branch (D_3) followed.

Acknowledgements

This work was funded by Harvard University, the Geological Survey of Namibia and a 1997 Carleton College Independent Research Fellowship entitled *Neoproterozoic tectonics and environments: An example from Namibia*. Additional research funds were provided by the 1997-1998 Carleton College Duncan Stewart Fellowship. Field observations were made by Farid Chemale, Ben Goscombe, Pippa Halverson, Charlie

Hoffmann, Paul Hoffman, Cees Paschier, Gaddy Soffer and Rudolph Trouw during the 1997 summer field season. Useful reviews of the manuscript were made by Guy Charlesworth, Ebbe Hartz, Alfred Kröner and Roy Miller. The author is indebted to Dave Bice, Bereket Haileab, Cin-ty Lee and John Shaw for many valuable discussions, and to Paul Hoffman for ongoing support since the earliest stages of this project.

References Cited

- Alvarez, W., Engleder, T. and Lowrie, W. 1976. Formation of spaced cleavage and folds in brittle limestone by dissolution. *Geology*, **4**, 698-701.
- Barnes, J.F.H. and Downing, K.N. 1979. Origin of domes in the central Damaran belt, Namibia. *Revue Géologie Dynamique et de Géographie Physique*, **21**, 383-386.
- Beck, M.E. 1998. On the mechanism of crustal block rotations in the central Andes. *Tectonophysics*, **299**, 75-92.
- Carey, S.W. 1955. The orocline concept in geotectonics, part 1. *Pap. Proc. R. Soc. Tasmania*, **89**, 255-288.
- Coward, M.P. 1981. The junction between Pan African mobile belts in Namibia: its structural history. *Tectonophysics*, **76**, 59-73.
- Coward, M.P. 1983. The tectonic history of the Damaran Belt. In: Miller, R. McG. (ed.) *Evolution of the Damara Orogen of South West Africa/Namibia. Spec. Publ. Geol. Soc. S. Afr.*, **11**, 409-421.
- Davis, G.H. and Reynolds, S.J. 1996. *Structural geology of rocks and regions*. John Wiley, New York, 776 pp.
- Dewey, J.F. 1988. Extensional collapse of orogens. *Tectonics*, **7**, 1123-1139.
- Dürr, S.B. and Dingledey, D.P. 1996. The Kaoko belt (Namibia): Part of a late Neoproterozoic continental-scale strike-slip system. *Geology*, **24**, 503-506.
- Fairchild, I.J. 1993. Balmy shores and icy wastes: the paradox of carbonates associated with glacial deposits in Neoproterozoic times. In: Wright, V.P., (ed.) *Sedimentology review*, Blackwell, Oxford, **1**, 1-16.
- Frets, D.C. 1969. Geology and structure of the Huab-Welwitschia area, South West Africa. *Bull. Precamb. Res. Unit, Univ. Cape Town*, **5**, 235 pp.
- Freund, R. 1970. Rotation of strike slip faults of Sistan, southeast Iran. *J. Geol.*, **78**, 188-200.
- Frimmel, H.E. and Frank, W. 1998. Neoproterozoic tectono-thermal evolution of the Gariiep Belt and its basement, Namibia and South Africa. *Precamb. Res.*, **90**, 1-28
- Germes, G.J.B. and Gresse, P.G. 1991. The foreland basin of the Damara and Gariiep orogens in Namaqualand and southern Namibia: stratigraphic correlations and basin dynamics. *S. Afr. J. Geol.*, **94**, 159-169.
- Gresse, P.G., Chemale, F., da Silva, L.C., Walvaren, F. and Hartmann, L.A. 1996. Late- to post-orogenic

- basin of the Pan-African-Brasiliano collision orogen in southern Africa and southern Brazil. *Basin Res.*, **8**, 157-171.
- Ghosh, S.K. 1970. A theoretical study of intersecting fold patterns. *Tectonophys.*, **9**, 559-569.
- Guj, P. 1970. The Damara mobile belt in the south-western Kaokoveld, South West Africa. *Bull. Precamb. Res. Unit, Univ. Cape Town*, **18**, 168 pp.
- Henry, G., Clendenin, C.W., Stanistreet, I.G. and Maiden, K. 1990. Multiple detachment model for the early rifting stage of the Late Proterozoic Damara orogen, Namibia. *Geology*, **18**, 67-71.
- Hoffman, P.F. 1991. Did the breakout of Laurentia turn Gondwanaland inside out? *Science*, **252**, 1409-1412.
- Hoffman, P.F. 1996. No SWEAT: Pan-African Damara Orogen (Namibia) as an unstable triple point, with implications for Rodinia. *GSA 28th Annual Abstracts with Programs*, 60-61.
- Hoffman, P.F., Kaufman, A.J., Halverson, G.P. and Schrag, D.P. 1998a. A Neoproterozoic snowball Earth. *Science*, **281**, 1342-1346.
- Hoffman, P.F., Kaufman, A.J. and Halverson, G.P. 1998b. Comings and goings of ice ages on a Neoproterozoic carbonate platform in Namibia. *GSA Today*, **8**(5), 1-9.
- Hoffman, P.F. 1999. The break-up of Rodinia, birth of Gondwana, true polar wander and the snowball Earth. *J. Afr. Earth Sci.*, **26**, 1-27.
- Hoffman, P.F., Halverson, G.P. and Soffer, G. 1999. Neoproterozoic glacial deposits and related carbonate sequences, Otavi Group, Namibia: A critical examination of evidence for a Neoproterozoic snowball earth. *Field Trip Guidebook (June 15-24, 1999), sponsored by The Can. Inst. for Advanced Research*, 29 pp.
- Hoffmann, K.H. 1983. Lithostratigraphy and facies of the Swakop Group of the southern Damara belt, SWA/Namibia. In: Miller, R. McG. (ed.) *Evolution of the Damara Orogen of South West Africa/Namibia*. Spec. Publ. Geol. Soc. S. Afr., **11**, 43-63.
- Hoffmann, K.H. 1989. New aspects of lithostratigraphic subdivision and nomenclature of late Proterozoic to early Cambrian rocks of the southern Damara belt and their correlation with the central and northern Damara belt and the Gariep belt. *Communs geol. Surv. Namibia*, **5**, 59-67.
- Kennedy, M.J. 1996. Stratigraphy, sedimentology, and isotopic geochemistry of Australian Neoproterozoic postglacial cap dolostones: deglaciation, $\delta^{13}\text{C}$ excursions, and carbonate precipitation. *J. Sed. Res.*, **66**, 1050-1064.
- Kennedy, M.J., Runnegar, J.B., Prave, A.R., Hoffmann, K.H. and Arthur, M. A. 1998. Two or Four Neoproterozoic glaciations? *Geology*, **26**, 1059-1063.
- Kröner, A. 1984. Dome structures and basement reactivation in the Pan-African Damara Belt of Namibia. In: Kröner, A. and Greiling, R., (eds) *Precambrian Tectonics Illustrated*, E. Schweizerbartische Verlagsbuchhandlung, Stuttgart, 191-206.
- Kukla, P.A. and Stanistreet, I.G. 1991. Record of the Damaran Khomas Hochland accretionary prism in central Namibia: Refutation of an "ensialic" origin of a Late Proterozoic orogenic belt. *Geology*, **19**, 473-476.
- Lisle, R.J., Styles, P. and Freeth, S.J. 1990. Fold interference structures: the influence of layer competence contrast. *Tectonophys.*, **172**, 197-200.
- McKenzie, D.P. and Morgan, W.J. 1969. Evolution of triple junctions. *Nature*, **224**, 125-133.
- Meert, J.G., Van der Voo, R. and Ayub, S. 1995. Paleomagnetic investigation of the Neoproterozoic Gage lavas and Mbozi complex, Tanzania and the assembly of Gondwana. *Precamb. Res.*, **74**, 225-244.
- Miller, R.McG. 1983. The Pan-African Damara orogen of South West Africa/Namibia. In: Miller, R. McG. (ed.) *Evolution of the Damara Orogen of South West Africa/Namibia*. Spec. Publ. geol. Soc. S. Afr., **11**, 431-515.
- Nelson, M.R. and Jones, C.H. 1987. Paleomagnetism and crustal rotations along a shear zone, Las Vegas Range, southern Nevada. *Tectonics*, **6**, 13-33.
- Nitsuma, N. 1996. The trench-trench-trench type triple junction and tectonic evolution of Japan. *Geosciences Reports of Shizuoka University*, **23**, 1-8.
- Nur, A., Hagai, R. and Scotti, O. 1986. Fault mechanics and the kinematics of block rotations. *Geology*, **14**, 746-749.
- Oliver, G.J.H. 1995. Mid-crustal detachment and domes in the central zone of the Damaran orogen, Namibia. *J. Afr. Earth Sci.*, **19**, 331-344.
- Passchier, C.W. and Trouw, R.A.J. 1996. *Micro-tectonics*. Springer-Verlag, Berlin, 289 pp.
- Porada, H. 1979. The Damara-Ribeira Orogen of the Pan-African-Brasiliano cycle in Namibia (South West Africa) and Brazil as interpreted in terms of continental collision. *Tectonophys.*, **57**, 237-265.
- Porada, H. 1989. Pan-African rifting and orogenesis in southern to Equatorial Africa and Eastern Brazil. *Precamb. Res.*, **44**, 103-136.
- Porada, H., Ahrendt, H., Behr, J. and Weber, K. 1983. The join of the coastal and intracontinental branches of the Damara Orogen, Namibia, South West Africa: In: Martin, H. and Eder, F.W. (eds) *Intracontinental Fold Belts*, Springer-Verlag, Berlin, 901-912.
- Prave, A.R. 1996. Tale of three cratons: Tectonostratigraphic anatomy of the Damara orogen in north-western Namibia and the assembly of Gondwana. *Geology*, **24**, 1115-1118.
- Ramsay, J.G. 1958. Superimposed folding at Loch Monar, Inverness-shire and Ross-shire. *Quat. J. geol. Soc.*, **113**, 271-307.
- Ramsay, J.G. 1962. Interference patterns produced by the superposition of folds of similar type. *J. Geol.*, **60**, 466-481.
- Ramsay, J.G. 1967. *Folding and fracturing of rocks*.

- McGraw-Hill Book Company, New York, 560 pp.
- Ramsay, J.G. and Huber, M.I. 1987. *The techniques of modern structural geology; v. 2: Folds and fractures*. Academic Press, London, 307 pp.
- Schmidt, P.W. and Williams, G.E. 1995. The Neoproterozoic climatic paradox: equatorial paleolatitude for Marinoan glaciation near sea level in South Australia. *Earth Planet. Sci. Lett.*, **134**, 107-124.
- Semikhatov, M.A. 1962. The Riphean and Lower Cambrian of the Yenisei mountains. *Trudy Geol. Inst. Akad. Nauk USSR*, **256**, 302p. (in Russian)
- Smith, D.A.M. 1965. The geology of the area around the Khan and Swakop Rivers in SW Africa. *Mem. geol. Surv. S. Afr., S.W. Afr. Series*, **3**, 113 pp.
- Stanistreet, I.G., Kukla, P.A., and Henry, G. 1991. Sedimentary basinal responses to a Late Precambrian Wilson Cycle: the Damaran Orogen and Nama Foreland, Namibia. *J. Afr. Earth Sci.*, **13**, 141-156.
- Sylvester, A.G. 1988. Strike-slip faults. *Bull. geol. Soc. Am.*, **100**, 1666-1703.
- Theissen, R.L. 1980. Classification of fold interference patterns; a reexamination. *J. struct. Geol.*, **2**, 311-316.
- Theissen, R.L. 1986. Two-dimensional re-fold interference patterns. *J. struct. Geol.*, **8**, 563-573.
- Thomas, W.A. 1983. Continental margins, orogenic belts, and intracratonic structures. *Geology*, **11**, 270-272.
- Thomas, W.A. 1990. Controls on the locations of transverse zones in thrust belts. *Eclogae Geologicae Helveticae*, **83**, 727-744.
- Tobisch, O.T. 1966. Large-scale basin-and-dome pattern resulting from the interference of major folds. *Bull. geol. Soc. Am.*, **77**, 393-408.
- Vauchez, A., Tommasi, A., and Egydio-Silva, M. 1994. Self-indentation of a heterogeneous continental lithosphere. *Geology*, **22**, 967-970.
- Watkinson, A.J. 1981. Patterns of fold interferences: influence of early fold shapes. *J. struct. Geol.*, **3**, 19-23.
- Weber, K., Ahrendt, H., and Hunziker, J.C. 1983. Geodynamic aspects of structural and radiometric investigations on the northern and southern margins of the Damara orogen, South West Africa/Namibia. *Spec. Publ. geol. Soc. S. Afr.*, **11**, 307-319.
- Weiss, L.E. 1959. Geometry of superposed folding. *Bull. geol. Soc. Am.*, **70**, 91-106.